Combined geophysical techniques for detailed groundwater flow investigation in tectonically deformed fractured rocks

John Alexopoulos[1], Emmanuel Vassilakis[1], Spyridon Dilalos[1]

[1] National and Kapodistrian University of Athens, University of Athens, Faculty of Geology and Geoenvironment, Kapodistrian, Panepistimiopolis, Greece

ABSTRACT

In this paper we present a combination of several near surface geophysical investigation techniques with high resolution remote sensing image interpretations, in order to define the groundwater flow paths and whether they can be affected by future seismic events. A seasonal spring (Amvrakia) located at the foot of Meteora pillars near the village of Kastraki (Greece) was chosen as a test site. The Meteora conglomeratic formations crop out throughout the study area and are characterized by large discontinuities caused by post Miocene till present tectonic deformation [Ferriere et al. 2011, Royden and Papanikolaou 2011]. A network of groundwater pathways has been developed above the impermeable marls underlying the conglomeratic strata. Our research aims to define these water pathways in order to investigate and understand the exact mechanism of the spring by mapping the exposed discontinuity network with classic field mapping and remote sensing image interpretation and define their underground continuity with the contribution of near surface geophysical techniques. Five Very Low Frequency (VLF) profiles were conducted with different directions around the spring aiming to detect possible conductive zones in the conglomeratic formations that the study area consists of. Moreover, two Electrical Resistivity Tomography (ERT) sections of a total length of 140m were carried out parallel to the VLF profiles for cross-checking and verifying the geophysical information. Both techniques revealed important conductive zones (<200 Ohm m) within the conglomerate strata, which we interpret as discontinuities filled with water supplying the spring, which are quite vulnerable to displacements as the hydraulic connections between them might be easily disturbed after a future seismic event.

1. Introduction

The research area is located at the southwest foot of Meteora pillars area and more specifically southeast of the Kastraki village (in Greece), where Amvrakia spring is found. Due to the fact that during the summer the spring suspends its function, our primary aim was to define its water capacity and its hydrogeological sensitivity to ground displacements since the area is not far (less than 20 km) from historical and contemporary earthquake epicenters [Papadimitriou and Karakostas 2003]. The study area is surrounded by almost vertical bluffs consisted of the Meteora molassic conglmer-atic for-
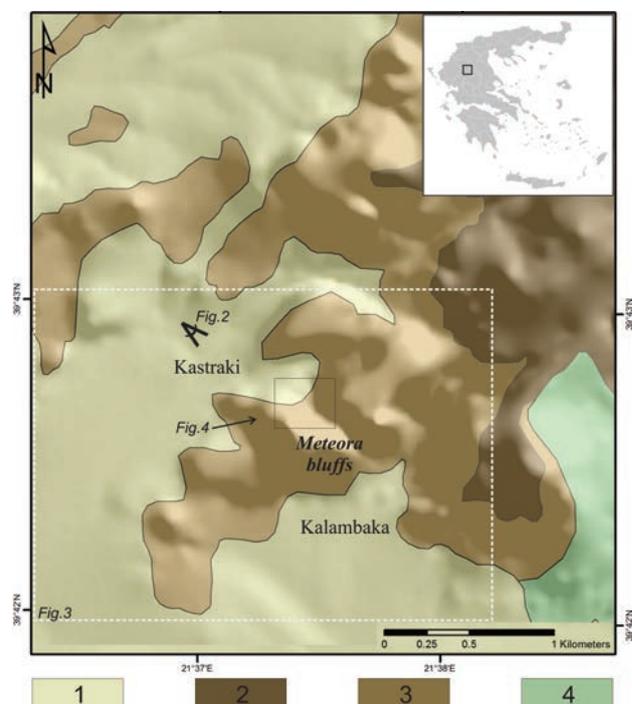

Figure 1. A simplified geological map of the surrounding area (marked at the inset map of Greece) draped on a shaded relief showing the impressive contrast of the topography is displayed, with the molassic conglomeratic formations of Tsotili (2), Pentalofos (3) and Eptachori (4) cropping out and surrounded by Quaternary deposits (1). The location of the study area (continuous line, see Figure 4), the direction of the photograph at Figure 2 as well as the extent of Figure 3 (with the dashed line) are also marked.

mations (Figure 1) and several difficulties had to be overcome for establishing the equipment and applying the described geophysical techniques. The dense vegetation at the foot of the hills, where the spring is located, the increased arduous accessibility and the relatively intense relief were the most significant problems that needed to be solved during fieldwork. Taking into account that the spring's supplying mechanism would probably take advantage of the dense network of the semi-open discontinuities existing in the conglomeratic strata, we had to define the orientation of these water pathways. The geophysical investigation aimed to focus on the detection of conductive zones and therefore geoelectrical and electromagnetic methods such as ERT and VLF that are the most indicative geophysical techniques for such environments [Caputo

Figure 2. An aspect of the geomorphological features developed on the molassic strata is shown. The visible discontinuities of tectonic origin are crossing the stratigraphic bedding and allow the groundwater flow through selective pathways.

et al. 2003, Sharma and Baranwal 2005, Papadopoulos et al. 2008, 2010] were planned on several directions.

2. Field observations and remote sensing data interpretation

The Meteora bluffs (Figure 2) are located at the southern margin of the Oligo-Miocene Meso-Hellenic molassic basin and are consisting mainly of the Meteora conglomerates. The geomorphology of the area is rather unique and therefore remote sensing datasets can prove to be very helpful in conjunction with field observations and structural measurements. [Ori and Roveri 1987] mention that the Meso-Hellenic basin is consisted of Gilbert-type delta deposits and deep chan-nel fills. They describe in detail the geometry of the sedimentary sequences of Meteora conglomerate, consisted mainly of transferred pebbles probably due to the erosion of several units composing the alpine orogene of the Hellenides [Papanikolaou 2009, Ferriere et al. 2011]. At the area of the bluffs, three out of the five units of the Meso-Hellenic molassic basin can be identified [Brunn 1956, Ferriere et al. 2004], while the stratigraphy of the study area is comprised of 3 different formations.

(1) The deepest formation is part of the transgressive succession of Eptachorion unit consisting of impermeable grey-blue marls of Upper Oligocene age (600 m thickness).

(2) Above these marls, massive conglomerate (700 m thickness) appears normally overlying [Brunn 1956, Papanikolaou et al. 1988], consisting of pebbles up to 20cm in diameter and originated from ophiolithes, marbles, limestones and metamorphic rocks in a sandy matrix. These massive crossed layered conglomerates have been deposited during Aquitanian [Brunn 1956] and are considered to be the southern outcrops of Pentalofos unit (which can be found further north of the study area). It is the material that the impressive pillars are comprised of and is known as the Meteora conglomeratic strata, which are gently dipping westwards [Ori and Roveri 1987]. The uppermost part of the formation consists of well-bedded sandstones.

(3) The upper formation of the area consists of disorganized conglomerates (100 m thickness) and is deposited above the Meteora conglomeratic strata through an angular unconformity [Ferriere et al. 2004, 2011]. It is quite often for these outcrops to be found at the highest elevations of the pillars and it is the lowest member of Tsotyli unit (of Burdigalian age) also known as the Upper Conglomerate of Meteora [Ori and Roveri 1987]. Several generations of structural discontinuities have been observed throughout the area of Meteora and are attributed to a large number of tectonic episodes during and after the Meso-Hellenic molassic basin evolution, which took place between Upper Eocene and Lower Miocene [Brunn 1956, Savoyat et al. 1972, Ferriere et al. 2004]. The general trending orientation of these almost vertical and open discontinuities is between N040E and N080E. Their hydrogeological significance is that they usually allow the water flow [Alexopoulos et al. 2011] but in many cases the sudden motion along them is responsible for groundwater level changes especially after seismic events [Marcaccio and Martinelli 2012, Gosar 2012]. The underlying impermeable marls of Eptachorion unit do not further allow the vertical infiltration of the groundwater since the flow happens within the discontinuities of the overlying conglomerates. A high spatial resolution (1 meter) pansharpened, multispectral IKONOS-2 satellite image dataset acquired during 2007 was combined with large scale topographic maps (1/5000), which were used as a base map. A Digital Elevation Model of 5 meter spatial resolution was used for ortho-rectifying the remote sensing dataset in order to use it for detailed mapping the surface exposure of the discontinuities and high accuracy measurements. Various image interpretation techniques, including spectral band combination and band ratios, led to the construction of a lineament map with morpho-lineaments [Vassilakis 2006], which refer to linear

features that are related either to the surface expression of tectonic structures or geomorphic features. In most cases
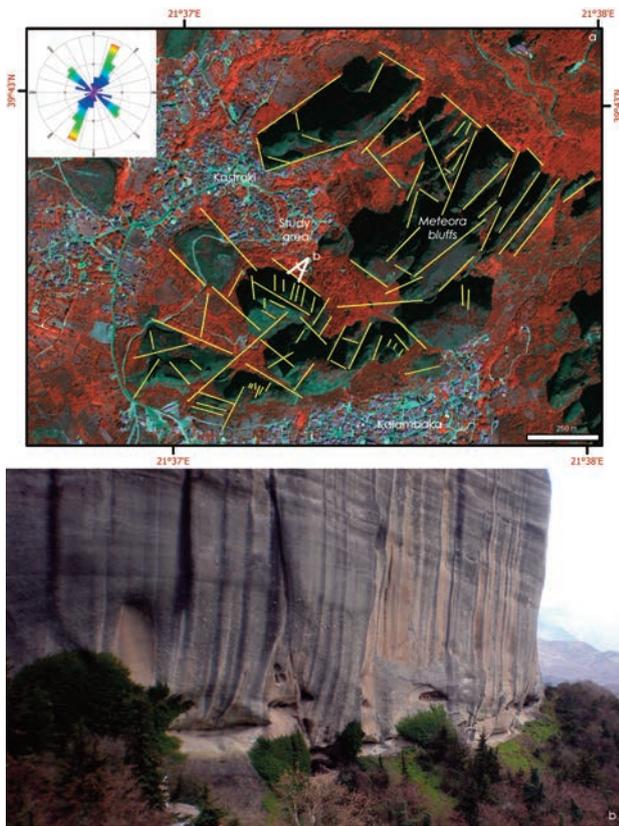

Figure 3. (a) Photogrammetric interpretation of an IKONOS-2 satellite image (4,2,3 - R,G,B) led to a photo-lineament map of the surrounding bluffs hosting the studied spring (Amvrakia). The inset rose-diagram is a result of the statistical interpretation of the lineaments' strike frequency. (b) Most of the lineaments are surface expressions of faults such as the one shown in this figure, displacing the strata of the Meteora conglomerates for tenths of centimeters.

they are relevant to post deposition tectonic activity. The 4,2,3 (R,G,B) band combination of the IKONOS image along with image enhancement techniques proved to be the most useful one (Figure 3), as different types of vegetation were highlighted and some of them delineate tectonic structures most of which were verified during field work. In this interpretation taller trees with high chlorophyll content are represented as red and create high contrast with shrub vegetation (brown), which in most cases in this area is located above the existence of groundwater. Therefore mapping this type of vegetation with multi-spectral remote sensing images can be very useful for detecting features that are related to structures of tectonic origin. The statistical interpretation of these features showed two main trends (NE and NW) that are in agreement with the field observations during which we measured several fault planes at the wider surrounding area. The measured throw of the faults varied from centimeters to

tenths of meters. Most of the displacements can be estimated as post-Aquitanian and in many cases post-Burdigalian, since the uppermost formation strata were also displaced by some of these faults or even more recent as the deep incision throughout the study area implies high uplift rates and consequently neotectonic activity, even though no clear marginal fault scarps were identified [e.g. Burbank and Pinter 1999 and references within]. Therefore, it is rather possible to observe displacements along these discontinuity planes in conjunction to a number of secondary phenomena (rockfalls, changes in groundwater circulation etc.) after a future seismic sequence, as quite a few earthquakes with M≥6.0 have occurred the last five centuries at the surrounding area [Papadimitriou and Karakostas 2003].

3. Electrical Resistivity Tomography (ERT)

The morpho-lineament map and the field observations led to the definition of a plan for the initial directions for ERT sections. The dense vegetation slightly altered the desired orientation with no particular impact on the final results (Figure 4). Two ERT sections trending normally to each other were carried out with a total length of 140 m. A 41 electrode array was established for applying the Wenner array configuration (190 measurement points of apparent resistivity) with electrode spacing up to 2 m. Topographic leveling measurements along the ERT sections were also carried out with high accuracy Real Time Kinematics Global Positioning System (RTK-GPS) equipment, since it is rather important to record the morphology as precisely as possible along the three axis (x,y,z). The overall methodology includes high precision measured elevation (+/- 0.01 meters) for each electrode since this is a great contribution to minimize the errors during the signal interpretation especially for groundwater investigations [Johnson et al. 2012]. The ERT measurements were processed with the RES2DINV software of GeoTomo. The raw resistivity data along with the topographic profile measurements for each transverse were imported into the software since the topographic correction was an important factor due to the intense relief of the study area. The inverse 2D model resistivity sections, derived from this interpretation and the processing results are quite impressive and detailed.

The first section (ERT-1) was chosen to be established between the two conglomeratic pillars, which are possibly supply the spring and at slightly higher elevations. The center of the electrode array was placed just uphill the spring location (Figure 5). The initial thought was to capture the main groundwater pathway and record the exact resistivity val-
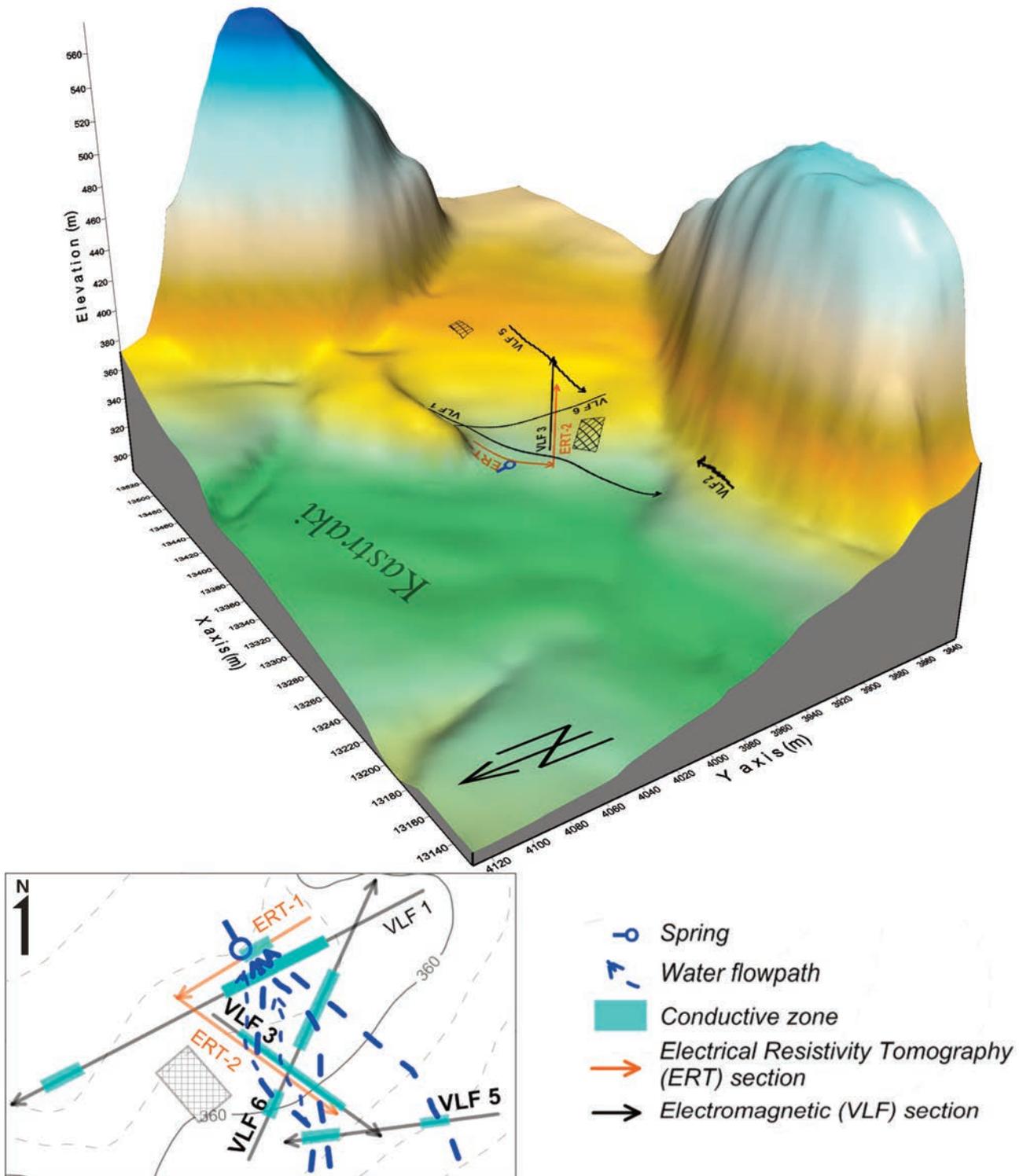
Figure 4. A 3-dimensional perspective representation of the study area on which the ERT and the VLF geophysical transverses are indicated. A 2-dimensional map of the same area along with the interpreted conductive zones and the groundwater flow paths is displayed below.

ues. After the interpretation a conductive (<200 Ohm m) curvy area has been revealed in the center of the section (25-35 m), beneath the spring, which is compatible with an overflow spring mechanism. A smaller conductive zone of the same resistivity values seems to exist further to the SW at the distance of 20 m from the spring, but its hydraulic connection to the main supplying pathway is not clear.

Therefore, a second electrode array was established (ERT-2) trending normally to the first one and uphill from the spring, aiming to capture several discontinuities that are used by the groundwater as pathways to the spring. Two parallel conductive zones (<200 Ohm m) at several depths have been detected after the interpretation (Figure 6). The topographic correction of the section was very significant as it became
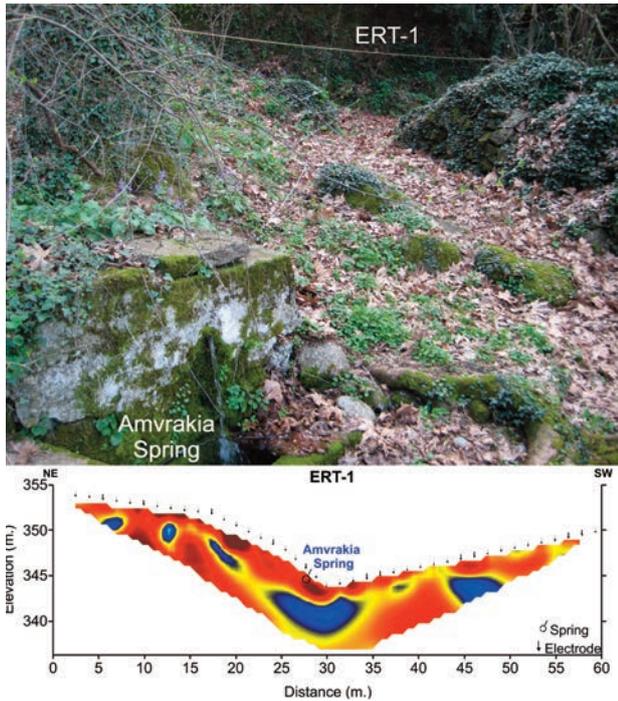
Figure 5. The first geoelectrical transverse was established uphill the spring location (above) and the interpreted tomography section, including topographic relief (below) revealed several conductive zones of relatively low resistivity values (ERT-1: 10th iteration, RMS: 2.38%). See Figure 6 for scale values.
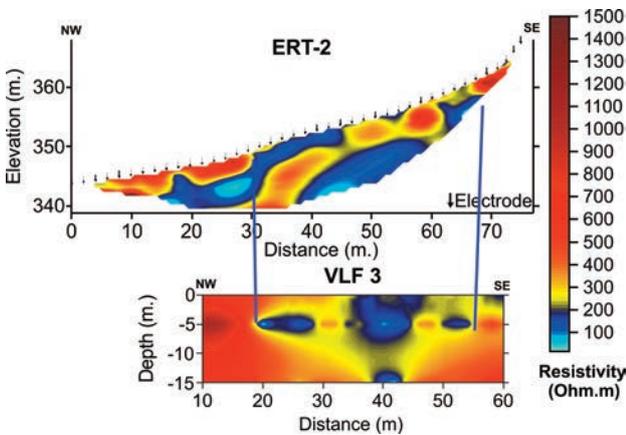

Figure 6. Comparison of resistivity sections generated from the inversion of the ERT-2 data values (11th iteration, RMS: 2.74%) and the VLF-3 data inversion with Inv2DVLF. It is clear that both the techniques have produced similar results.

rather clear that both of the zones are gently dipping towards the spring and this could be interpreted as water-bearing discontinuities of the conglomerates.

4. Very Low Frequency Electromagnetic Survey (VLF)

The VLF technique was performed in order to validate the conductive zones, detected by ERT measurements in higher detail. In many cases VLF measurements are proved to be ideal for detecting vertical to sub-vertical conductive zones or possible karst structures mainly for hydrogeological investigation purposes
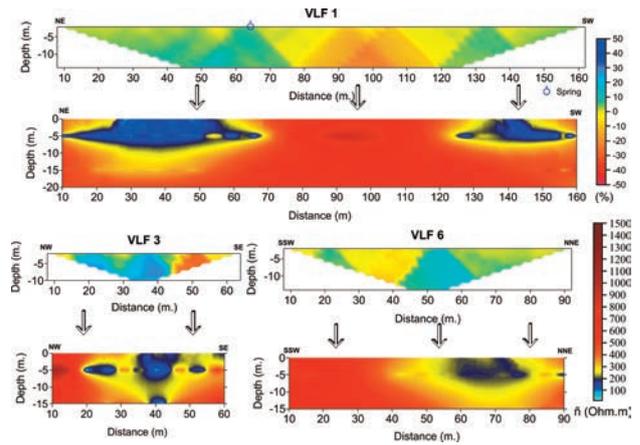

Figure 7. The Karous-Hjelt pseudo-sections of the selected profiles VLF 1, VLF 3 and VLF 6 are represented. The respective resistivity section derived from inversion with Inv2DVLF software is also included (Initial resistivity 500 Ohm.m with 20 iterations. RMSVLF 1= 1.16%, RMSVLF 3=1.82%, RMSVLF 6=0.95%). Frequency: 23.4 KHz.

[Monteiro-Santos 2006, Papadopoulos et al. 2008, Sharma and Baranwal 2005, Dilalos 2009, Alexopoulos et al. 2011]. By applying this methodology, the lateral and vertical resistivity distribution is investigated. Based on the field mapping, the statistical analysis of the morpho-lineaments and the orientation of the exposed fractures, five profiles were conducted (Figures 6, 7). Two of them (VLF1 and VLF3) were designed to partially cover the ERT sections and consequently validate those results by com-bining the measurements from both geophysical methods. The rest of them were conducted along several directions around the spring's area, aiming to either detect the extension of the already mapped conductive zones or reveal new unexposed water-bearing discontinuities at the conglomeratic strata.

The spacing of the measurement stations along the section was 2 meters, as a high detailed investigation needed to be carried out. A main VLF source frequency of 23.4 KHz was used, due to the good signal and alignment, towards the direction of the expected anomalies (westwards inclination). The processing of the VLF profiles included smoothing of the raw data and topographic corrections, according to Baker and Myers [1980] and Eberle [1981]. Afterwards, we applied the Fraser [1969] and Karous-Hjelt filters [Karous 1979, Karous and Hjelt 1983], both of which spotlight the anomalies. Karous-Hjelt filter provides information of relative current density distribution with depth by producing the pseudo-sections (semi-quantity interpretation) (Figure 7). At VLF 1 pseudo-section, a main conductive zone is located be-tween 30-75 m after the starting point, probably due to the spring (located at 65 m) and a smaller one at 125-140 m. The interpretation of VLF 3 pseudo-section reveals a conductive zone at 25-55 m, whilst at VLF 6 pseudo-section a main con-

ductive zone between 40-70 m and a smaller one at 15-30 m are indicated (Figure 4, 7).

Additionally, the VLF measurements were processed with Inv2DVLF inversion software presented by Monteiro-Santos [2006, 2007]. The software is in general an algorithm that inverts normalized VLF data with the method of smoothed least-squares, based on the scalar tipper originated from the relation of vertical and horizontal component of the magnetic field. The result of this procedure is the subsurface distribution of the resistivity and has proved to give reliable results similar to those of detailed geoelectrical measurements [Monteiro-Santos et al. 2006, Dilalos 2009]. The resistivity profiles extracted by this procedure are illustrated in Figure 7 below each Karous-Hjelt pseudo-section, representing the same conductive zones (<200 Ohm m), highlighted according to the color scale. The initial resistivity chosen for the in-version (20 iterations according to the software's author) was 500 Ohm m, based on the dominant resistivity of the con-glomerates [Alexopoulos et al. 2005].

5. Discussion - Conclusions

Both of the geophysical techniques applied for this study proved to be ideal for indicating conductive zones. The results of the comparison between the two techniques along the same transverse are represented at Figure 6. The resistivity section generated by the inversion of the ERT-2 data compared to the resistivity section generated by the VLF-3 data inversion using the Inv2DVLF algorithm are surprisingly very well related. The ERT section, obviously illustrates the conductive zones in higher detail than the VLF measurements, but it is rather clear that along these two sections, where we applied both ERT and VLF measurements, we had the opportunity to detect the exact same conductive zones, confirming and validating the results.

High resolution remote sensing data interpretation and ground truth field observations proved to be very useful in planning the preferable geophysical transverse orientation, considering the vegetation density as well. Since the area is comprised of massive conglomeratic strata, which are formations of high resistivity (>500 Ohm m) [Alexopoulos et al. 2005], we were able to identify the conductive zones (<200 Ohm m) as the most probable underground water pathways and relate them to the observed discontinuities, trending towards the Amvrakia spring. At the ERT-2 section gentle dipping of these underground pathways to north-west is indicated (better shown on ERT section - Figure 6) towards the location of the spring, whilst at the section of ERT-1 a local concavity is represented, which verifies the mechanism of an overflow spring. The conductive zones along with the delineated water pathways (Figure 4) leading towards the spring are in full correspondence to the discontinuities of the arising Meteora conglomerate pillars (Figure 4).

It is noteworthy that the groundwater pathways that supply the spring are quite many but not very extensive throughout the uphill area. Additionally, the geophysics interpretations show that the crucial for the spring operation conductive zones are detected at relatively shallow depths, although the hosting discontinuities should extend much deeper than that. On top of that, at this rather sparse discontinuity network we observed displacement at several of them and a sig-nificant number of these fault surfaces seem to have the potential to be easily reactivated, especially as a secondary phenomenon after a future seismic event at a relatively close epicenter area. During this case scenario the water supply might suffer changes that could reduce either the supply or the spring operation time space.

References

Alexopoulos, J., S. Dilalos and E. Vassilakis (2011). Adumbration of Amvrakia's spring water pathways, based on de-tailed geophysical data (Kastraki-Meteora). In: N. Lambrakis, G. Stournaras and K. Katsanou (Editors), Advances in the Research of Aquatic Environment. Springer, 105-112.

Alexopoulos, J.D., T. Papadopoulos and A. Mastroyannis (2005). Investigation of hydrogeological factors affecting the potable water wells of Kalampaka urban by using geophysical techniques. Proc. of the 7th Hellenic hydrogeological conference, 19-30.

Baker, H.A., and J.O. Myers (1980). A topographic correction for the VLF-EM profiles based on model studies. Geoex-ploration 18, 135-144.

Brunn, J.H. (1956). Etude geologique du Pinde septentrional de la Macedoine occidentale. Ann. Geol. Pays. Hellen. 7, 1-358.

Burbank, D. W., and N. Pinter (1999). Landscape evolution: the interactions of tectonics and surface processes. Basin Research, 11, 1-6.

Caputo, R., S. Piscitelli, A. Oliveto, E. Rizzo and V. Lapenna (2003). The use of electrical resistivity tomographies in active tectonics: examples from the Tyrnavos Basin, Greece. Journal of Geodynamics 36, 19-35.

Dilalos, S. (2009). Exploration of hydrogeological and

environmental conditions with geophysical techniques, at selected sites in Chios island (Greece) M.Sc Thesis. National and Kapodistrian University of Athens, Faculty of Geology and Geoenvironment. Athens.

Eberle, D. (1981). A method of reducing terrain relief effects from VLF-EM data. Geoexploration 19, 103-114.

Ferriere, J., F. Chanier, J.Y. Reynaud, A. Pavlopoulos, P. Ditbanjong, G. Migiros, I. Coutand, A. Stais and J. Bailleul (2011). Tectonic control of the Meteora conglomeratic formations (Mesohellenic basin, Greece). Bull. Soc. Geol. Fr. 182, 437-450.

Ferriere, J., J. Reynaud, A. Pavlopoulos, M. Bonneau, G. Migiros, F. Chanier, J. Proust and S. Gradin (2004). Geologic evolution and geodynamic controls of the Tertiary intramontagne piggyback Meso-Hellenic basin, Greece. Bull. Soc. Geol. Fr. 175/4, 361-381.

Ferriere, J., F. Chanier, J.Y. Reynaud, A. Pavlopoulos, P. Ditbanjong, G. Migiros, I. Coutand, A. Stais and J. Bailleul (2011). Tectonic control of the Meteora conglomeratic formations (Mesohellenic basin, Greece). Bull. Soc. Geol. Fr. 182, 437-450.

Fraser, D.C. (1969) Contouring of VLF-EM data. Geophysics 34/6, 958-967.

Gosar, A. (2012). Application of Environmental Seismic Intensity scale (ESI 2007) to Krn Mountains 1998 Mw =5.6 earthquake (NW Slovenia) with emphasis on rockfalls. Nat. Hazards Earth Syst. Sci. 12, 1659-1670.

Johnson, T. C., L.D. Slater, D. Ntarlagiannis, F. D. Day-Lewis and M. Elwaseif (2012). Monitoring groundwater-surface water interaction using time-series and time-frequency analysis of transient three-dimensional electrical re-sistivity changes. Water Resources Research, 48(7), W07506.

Karous, M. (1979). Effect of relief in EM methods with very distant source. Geoexploration 17, 33-42.

Karous, M., and S.E. Hjelt (1983). Linear filtering of VLF dip-angle measurements. Geophysical Prospecting 31, 782-794.

Marcaccio, M., and G. Martinelli (2012). Effects on the groundwater levels of the May-June 2012 Emilia seismic sequence, Annals of Geophysics, 55(4).

Monteiro-Santos, F.A. (2006). Instructions for running PrepVLF and Inv2DVLF; 2-D inversion of VLF-EM single fre-quency programs. Version 1.0. Lisboa.

Monteiro-Santos, F.A. (2007). New features PrepVLF and Inv2DVLF. Version 1.1. Lisboa.

Monteiro-Santos, F.A., Almeida E.P., Gomes M., and A. Pina (2006). Hydrogeological investigation in Santiago Island (Cabo Verde) using magnetotellurics and VLF methods. Journal of African Earth Sciences 45, 421-430.

Monteiro-Santos, F.A., A. Mateus, J. Figueiras and M.A. Concalves (2006). Mapping groundwater contamination around a landfill facility using the VLF-EM method-A case study. Journal of Applied Geophysics 60, 115-125.

Ori, G.G., and M. Roveri (1987). Geometries of Gilbert-type deltas and large channels in the Meteora Conglomerate, Meso-Hellenic basin (Oligo-Miocene), central Greece. Sedimentology 34, 845-859.

Papadimitriou, E.E, and V.G. Karakostas (2003) Episodic occurrence of strong (Mw≥6.2) earthquakes in Thessalia area (central Greece). Earth and Planetary Science Letters 215, 395-409.

Papadopoulos, T.D., J.D. Alexopoulos, S. Dilalos and M.J. Pippidis (2008). Resistivity and VLF measurements for spring mechanism determination at NE Chios Isl. Proc. of the 8th International hydrogeological congress of Greece, 337-346.

Papadopoulos, T.D., G. Stournaras and J.D. Alexopoulos (2010). Geophysical investigations for aquifer detection in fis-sured rocks of volcanic origin. A case history. Journal of the Balkan Geophysical Society 13/2, 1-8.

Papanikolaou, D. (2009). Timing of tectonic emplacement of the ophiolites and terrane paleogeography in the Helleni-des. Lithos 108, 262-280.

Papanikolaou, D.J, E.L. Lekkas, I.D. Mariolakos and R.M Mirkou (1988). Contribution to the geodynamic evolution of the Mesohellenic basin (in Greek). Bull. Geol. Soc. Greece 20, 17-36.

Royden, L.H., and D.J. Papanikolaou (2011). Slab segmentation and late Cenozoic disruption of the Hellenic arc. Geo-chem. Geophys. Geosyst. 12, Q03010.

Sharma, S.P., and V.C. Baranwal (2005). Delineation of groundwater-bearing fracture zones in a hard rock area integrat-ing very low frequency electromagnetic and resistivity data. Journal of Applied Geophysics 57, 155-166.

Savoyat, E., N. Lalechos, N. Philippakis and G. Bizon (1972). Geological map of Greece, scale 1:50.000, Kalambaka Sheet. Inst. Geol. and Miner. Explor., Athens.

Vassilakis, E. (2006). Study of the tectonic structure of Messara basin, central Crete, with the aid of remote sensing techniques and G.I.S. PhD Thesis, National & Kapodestrian University of Athens, Athens, 546 pp.

*Corresponding author: John Alexopoulos,
National and Kapodistrian University of Athens, Faculty of Geology and Geoenvironment, , Panepistimiopolis, Greece;
email: jalexopoulos@geol.uoa.gr